Supporting Information

Phosphorus vacancies improve hydrogen evolution of MoP electrocatalysts

Hui Ma, [a,b,#] Wensi Yan, [a,#] Yanlong Yu, [b] LiHua Deng, [a,b] Zhe Hong, [a] Li Song, [a,*] and Lei Li [a,*]

[a] College of Biological, Chemical Sciences and Engineering, Jiaxing University, Jiaxing, Zhejiang 314001, China

[b] College of Chemistry and Chemical Engineering, Northeast Petroleum University, Daqing, Heilongjiang 163318, China

[*] Corresponding author. E-mail: songli@mail.zjxu.edu.cn (L. Song); leili@mail.zjxu.edu.cn (L. Li)

# These authors contributed equally to this work.

Materials

Ammonium molybdate tetrahydrate ($(NH_4)_6Mo_7{\cdot}4H_2O$), acetone (CH_3COCH_3) and ethanol (C_2H_5OH) were purchased from Sinopharm Chemical Reagent Co., Ltd. Sodium dodecyl sulfonate (SDS, $NaC_{12}H_{25}SO_3$) and Sodium hypophosphite (NaH_2PO_2) were purchased from Shanghai Macklin Biochemical Technology Co., Ltd. Carbon cloth (CC) was purchased from CeTech Co., Ltd. All chemical reagents used in this experiment were of analytical grade and put to use without further purification.

Characterization

Powder XRD patterns of the as-synthesized samples were recorded by XRD-700 (SHIMADZU) X-ray diffractometer equipped with Cu-Kα (λ = 0.1541 nm) radiation operating at 40 kV and 40 mA with a scanning rate of 2 °/min. The X-ray photoelectron spectroscopy (XPS) measurements were performed on a VG ESCALAB 250 spectrophotometer with Al Ka radiation (1486.6 eV), operating at 15 kV × 10 mA, in FAT mode (Fixed Analyzer Transmission), with a pass energy of 30 eV for regions ROI and 100 eV for survey. The base pressure of the main chamber was kept at about 1×10^{-9} mbar. Each sample was first placed in a copper holder mounted on a sample-rod in the pretreatment chamber of the spectrometer, and it was then outgassed at 100 °C for 1 h before being transferred to the analysis chamber. A flood gun was always used for charge compensation. The spot size is 500 μm and each high-resolution spectrum was scanned for ten times with an energy step size of 0.05 eV. All binding energies (BE) were calibrated by using that of C 1 s (284.8 eV). The peaks obtained after a Shirley background subtraction were fitted to Lorentzian-Gaussian curves using a public software XPSPEAK version 4.1. High resolution transmission electron microscope images (HRTEM) and high angle annular dark field scanning transmission electron microscopy (HAADF-STEM) images were obtained using a ThermoFisher Talos F200x microscope. Raman spectra were collected at room temperature on a DXR2xi (ThermoFisher) instrument using a semiconductor laser as an illumination source (532 nm).

Electrochemically Active Surface Area

The electrochemically active surface area (ECSA) is a useful parameter to compare the active surface area and the electrochemically capacitance (C_{dl}) measurements were conducted by cyclic voltammograms from 0.0968 to 0.1968 V vs. RHE with various scan rates (20, 40, 60, 80, 100 mV s^{-1}).[1] The capacitive currents were measured in a potential where no faradic processes were observed (i.e., at 0.15 V vs. RHE). In addition, the slope of the Δj vs. scan rate curve is twice that of the C_{dl}.[2] According to the previous report, it is suitable that using a 40 μF cm^{-2} as the specific capacitance value. Thus, the A_{ECSA} can be calculated by the following formula:[3]

$$A_{ECSA} = \frac{\text{electrochemical capacitance}}{40\ \mu\text{F cm}^{-2}\ \text{per cm}^2_{ECSA}}$$

Calculated Electrochemically Active Surface Area

MoP:
$$A^{MoP}_{ECSA} = \frac{0.64\ \text{mF cm}^{-2}}{40\ \mu\text{F cm}^{-2}\ \text{per cm}^2_{ECSA}} = 16\ \text{cm}^2_{ECSA}$$

MoP-Pv:
$$A^{MoP-Pv}_{ECSA} = \frac{0.80\ \text{mF cm}^{-2}}{40\ \mu\text{F cm}^{-2}\ \text{per cm}^2_{ECSA}} = 20\ \text{cm}^2_{ECSA}$$

Turnover frequency calculations

The turnover frequency can be calculated by the following formula:

$$\text{TOF} = \frac{\#\text{total hydrogen turn overs /cm}^2\ \text{geometricarea}}{\#\text{activesites /cm}^2\ \text{geometricarea}}$$

The total number of hydrogen turn overs was calculated from the current density according to:[4,5]

$$\#_{H_2} = \left(\text{j}\frac{\text{mA}}{\text{cm}^2}\right)\left(\frac{1\text{C s}^{-1}}{1000\ \text{mA}}\right)\left(\frac{1\ \text{mol e}^-}{96485\ \text{C}}\right)\left(\frac{1\ \text{mol H}_2}{2\ \text{mol e}^-}\right)\left(\frac{6.022\times10^{23}\text{H}_2\ \text{molecules}}{1\ \text{mol H}_2}\right)$$

$$= 3.12\times10^{15}\ \frac{\text{H}_2\text{/s}}{\text{cm}^2}\ \text{per}\frac{\text{mA}}{\text{cm}^2}$$

Active sites per real surface area

$$\text{MoP:} \quad \#\text{active sites} = \left(\frac{2 \text{ atoms/unit cell}}{28.7 \text{ Å}^3\text{/unit cell}}\right)^{\frac{2}{3}} = 1.69 \times 10^{15} \text{ atoms cm}_{\text{real}}^{-2}$$

Finally, plot of current density can be converted into a TOF plot according to

$$\text{TOF} = \frac{(3.12 \times 10^{15} \frac{\text{H}_2\text{/s}}{\text{cm}^2} \text{per} \frac{\text{mA}}{\text{cm}^2}) \times |j|}{\#\text{active sites} \times A_{ECSA}}$$

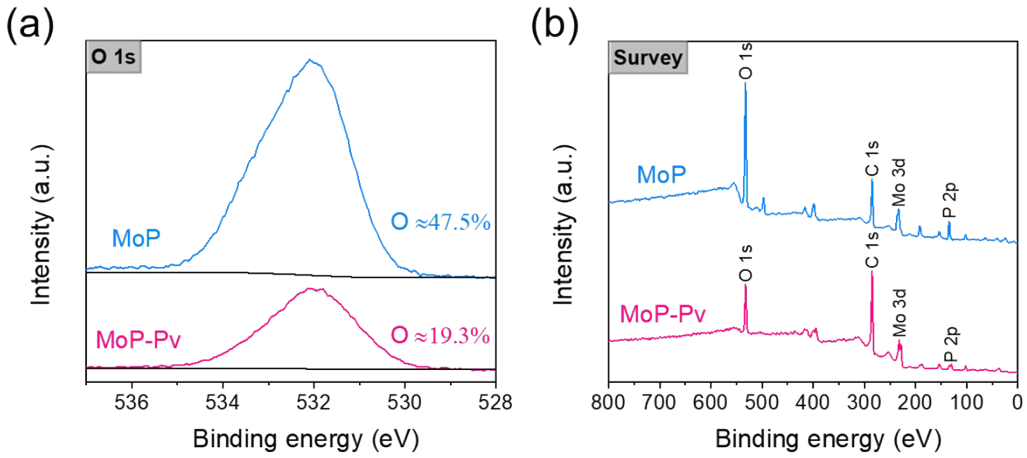

Fig. S1. (a) XPS spectrum of O 1s in MoP and MoP-Pv; (b) XPS full spectrum of MoP and MoP-Pv.

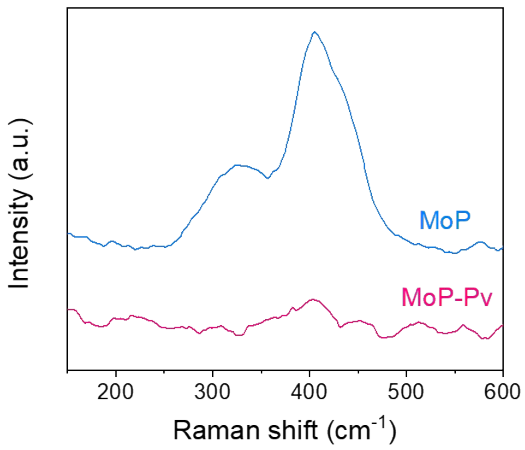

Fig. S2. Raman spectra of MoP and MoP-Pv.

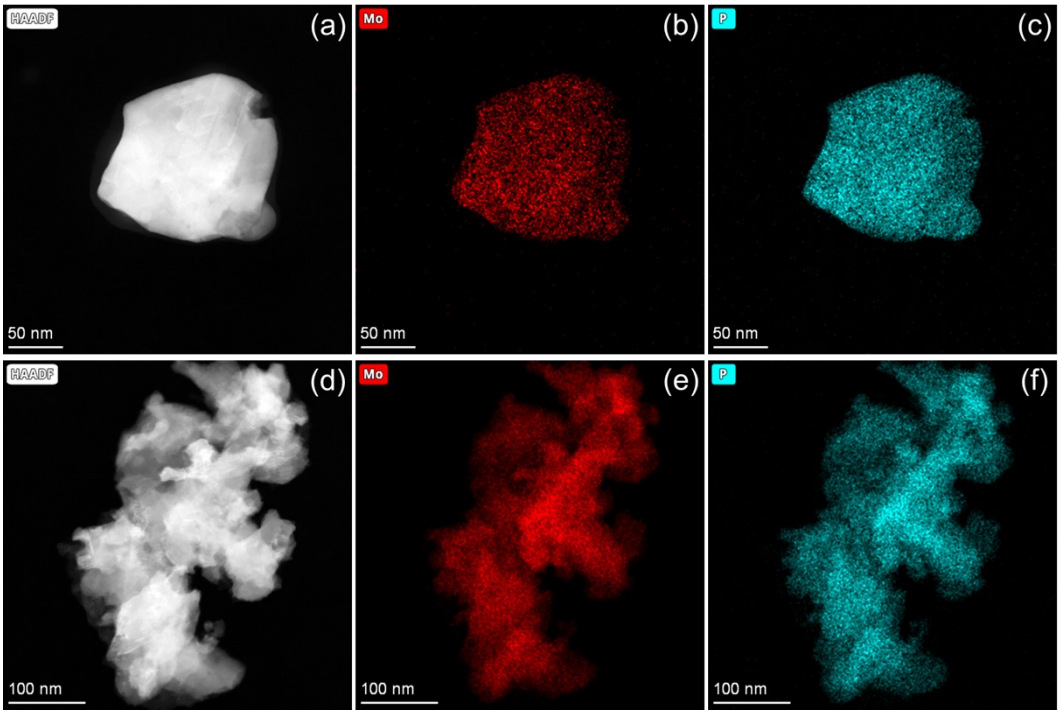

Fig. S3. Elemental mapping of Mo and P from MoP (a,b,c) and MoP-Pv (d,e,f).

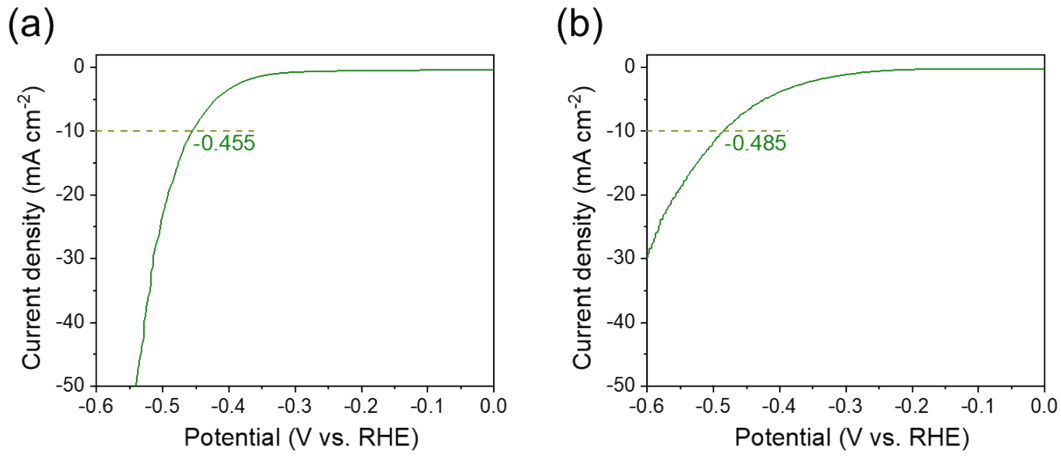

Fig. S4. Polarization curves of MoO_2 in (a)1 M KOH solution; (b) 0.5 M H_2SO_4 solution.

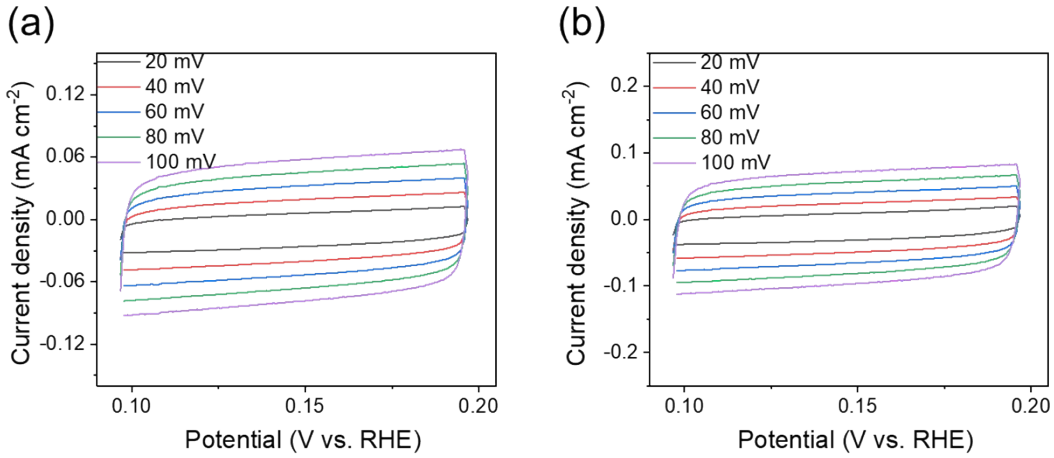

Fig. S5. Cyclic voltammetry curves of (a) MoP and (b) MoP-Pv samples from 0.0968 to 0.1968 V vs. RHE at various scan rates from 20 to 100 mV·s^{-1} in 1 M KOH solution.

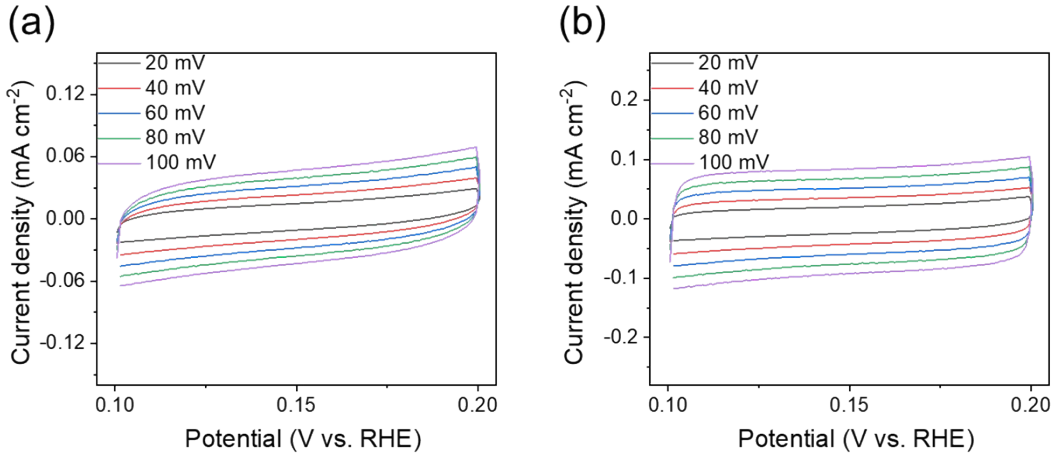

Fig. S6. Cyclic voltammetry curves of (a) MoP and (b) MoP-Pv samples from 0.1015 to 0.2015 V vs. RHE at various scan rates from 20 to 100 mV·s^{-1} in 0.5 M H_2SO_4 solution.

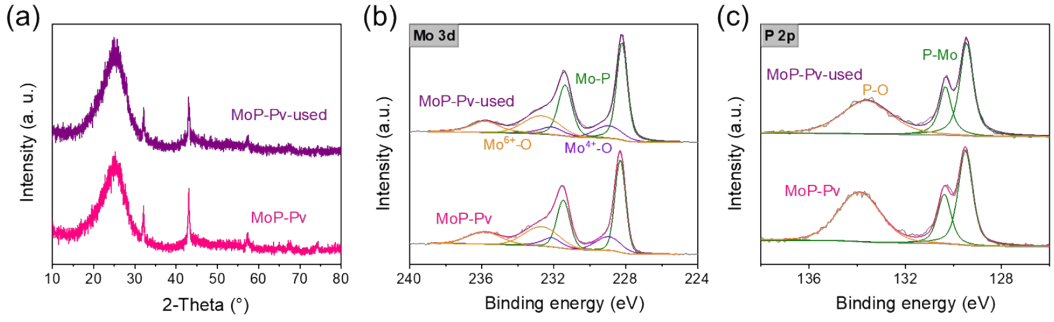

Fig. S7. (a) XRD patterns and high-resolution XPS spectra of (b) Mo 3d, (c) P 2p of MoP-Pv and MoP-Pv after the durability test.

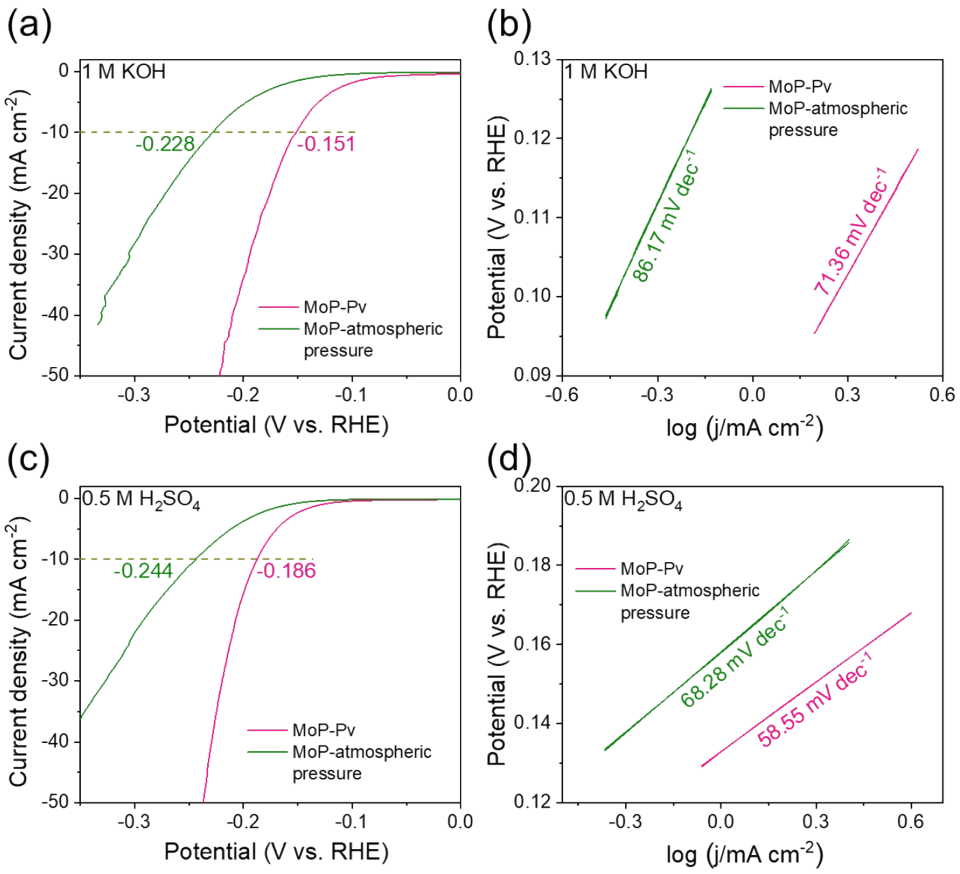

Fig. S8. (a) Polarization curves and (b) Tafel plots of MoP-Pv generated under vacuum and MoP prepared by hydrogen annealing under atmospheric pressure in 1 M KOH solution; (c) Polarization curves and (d) Tafel plots of MoP-Pv generated under vacuum and MoP prepared by hydrogen annealing under atmospheric pressure in 0.5 M H_2SO_4 solution.

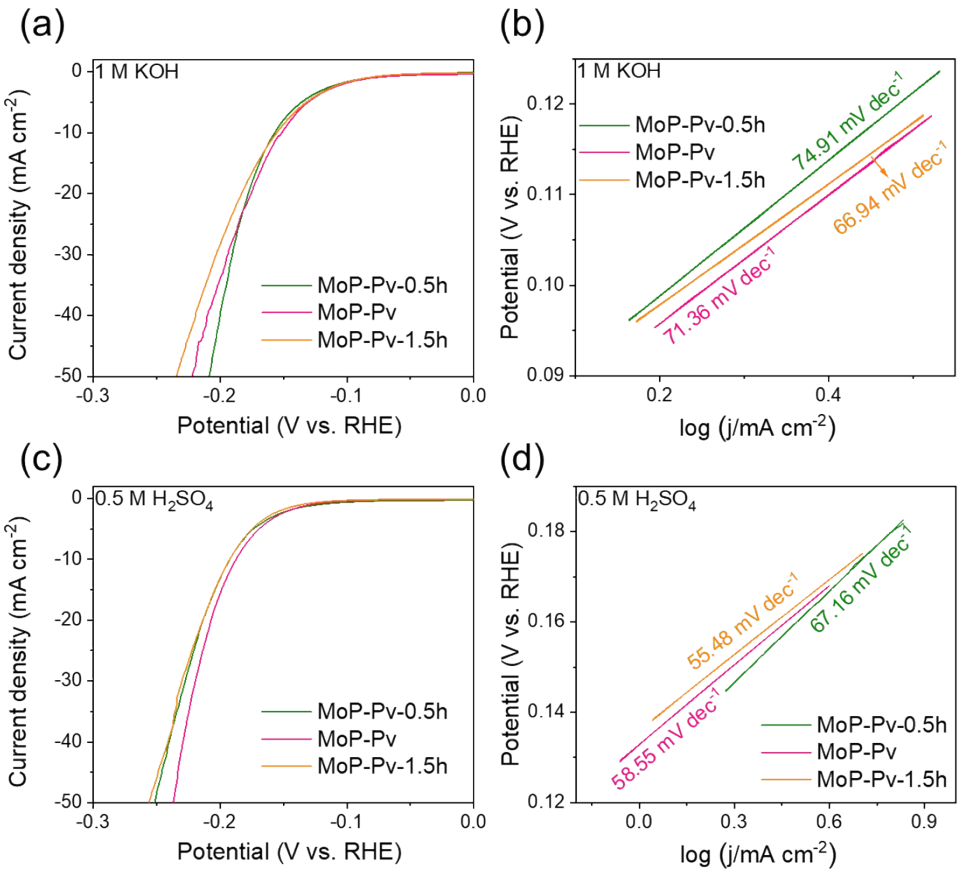

Fig. S9. (a) Polarization curves and (b) Tafel plots of MoP-Pv generated by different duration of hydrogen reduction in 1 M KOH solution; (c) Polarization curves and (d) Tafel plots of MoP-Pv by different duration of hydrogen reduction in 0.5 M H_2SO_4 solution.

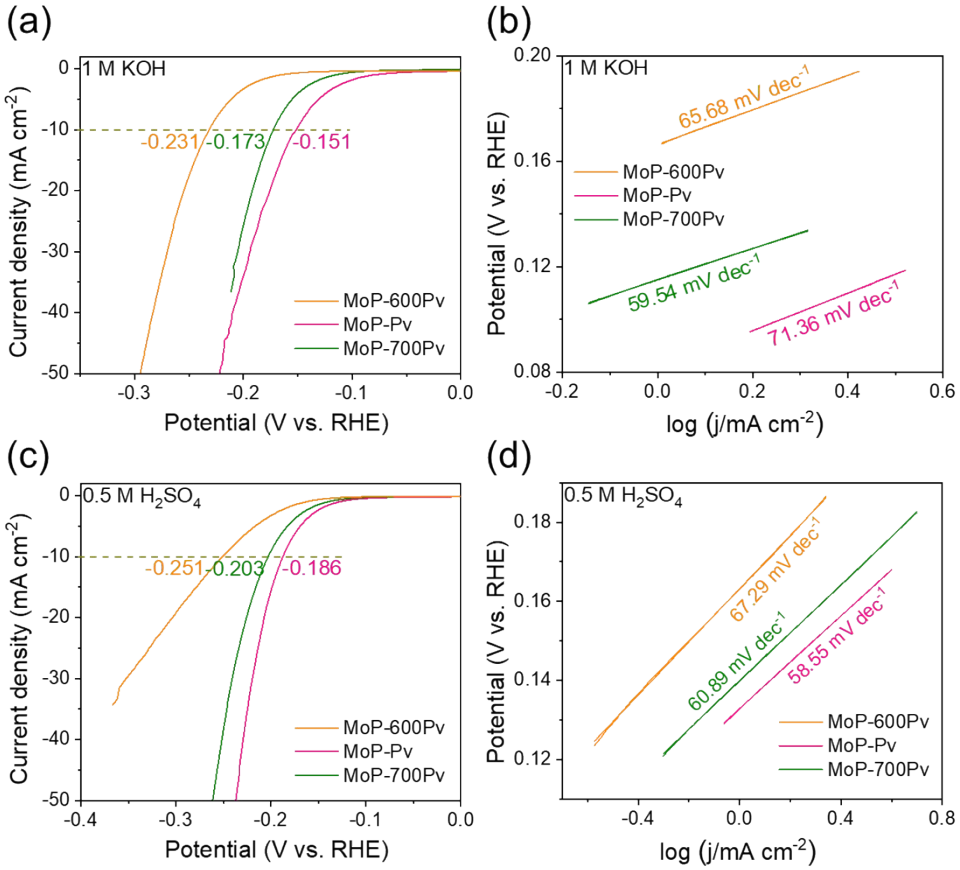

Fig. S10. (a) Polarization curves and (b) Tafel plots of MoP-Pv generated by different temperature in 1 M KOH solution; (c) Polarization curves and (d) Tafel plots of MoP-Pv generated by different temperature in 0.5 M H_2SO_4 solution.

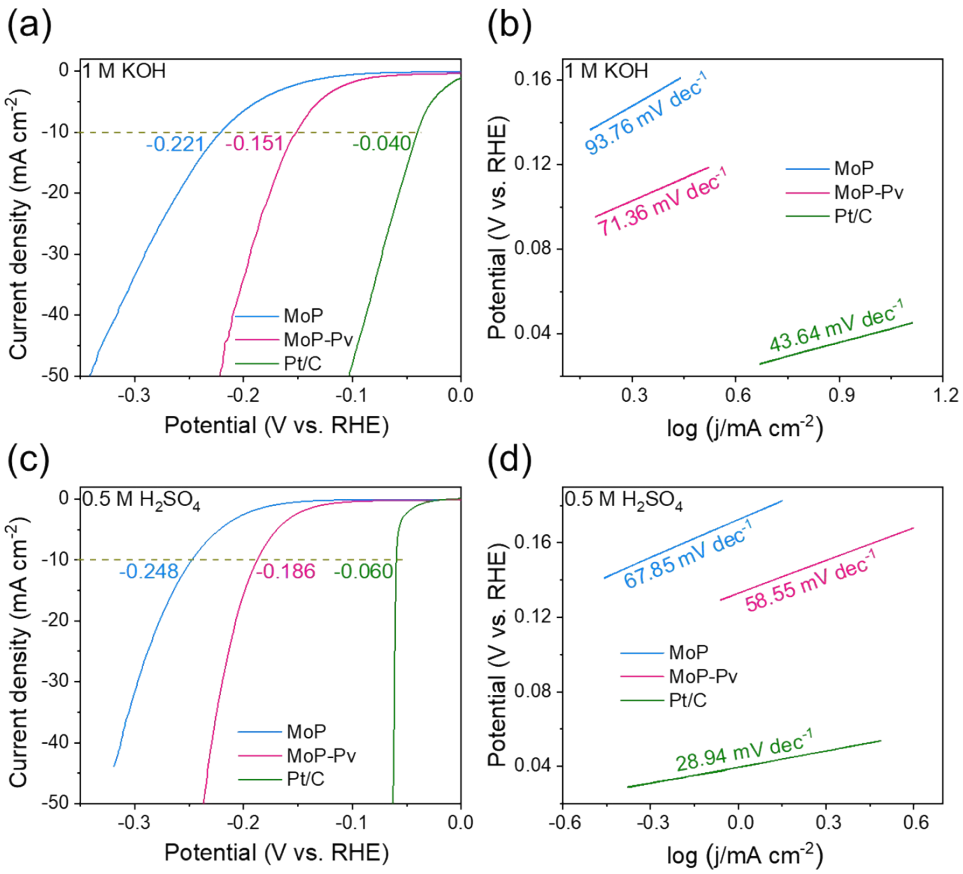

Fig. S11. (a) Polarization curves and (b) Tafel plots of MoP, MoP-Pv and Pt/C in 1 M KOH solution; (c) Polarization curves and (d) Tafel plots of MoP, MoP-Pv and Pt/C in 0.5 M H_2SO_4 solution.

Table. S1. Comparison of HER performance with other MoP-based HER electrocatalysts.

Catalysts	electrolyte	η at 10mA·cm^{-2} (mv)	Ref.
MoP-Pv	1 M KOH	-151	This work
	0.5 M H_2SO_4	-186	
0.02Ni-MoP	1 M KOH	-162	*Nano Energy*, 2020, **70**, 104445.
	0.5 M H_2SO_4	-102	

La-MoP@NC	1 M KOH	-136.5	*Appl. Catal. B*, 2021, **299**, 120657.
	0.5 M H_2SO_4	-142.18	
MoP@NPCS	1 M KOH	-172	*Appl. Catal. B*, 2020, **263**, 118352.
	0.5 M H_2SO_4	-113	
MoP@NC	1 M KOH	-149	*Appl. Catal. B*, 2020, **263**, 118358.
	0.5 M H_2SO_4	-96	
Mn-MoP	1 M KOH	-210	*Appl. Surf. Sci.*, 2021, **551**, 149321.
	0.5 M H_2SO_4	-199	
MoP/NC	1 M KOH	-213	*ACS Appl. Energy Mater.*, 2021, **4**, 5486-5492.
	0.5 M H_2SO_4	-183	
N@MoPCx nanosheet	1 M KOH	-139	*Adv. Energy Mater.*, 2018, **8**, 1701601.
D-MoP/rGO	1 M KOH	-122	*Inorg. Chem. Front.*, 2019, **6**, 2686.
	0.5 M H_2SO_4	-138	
N-MoP-800	1 M KOH	-125	*Electrochim. Acta*, 2020, **342**, 136059.
	0.5 M H_2SO_4	-175	
MoP/ NC	1 M KOH	-170	*Appl. Catal. B*, 2019, **245**, 656-661.
	0.5 M H_2SO_4	-120	
DR-MoP	1 M KOH	-104	*Electrochim. Acta*, 2018, **281**, 540-548.
	0.5 M H_2SO_4	-156	
G6.0U2.0Mo4.0	1 M KOH	-103	*New J. Chem.*, 2022, **46**, 12461.
	0.5 M H_2SO_4	-145	
MoP@NPC-1.0	1 M KOH	-134	*J. Alloys Compd.*, 2022, **929**, 167254.

Co-1.5 h-MoP	0.5 M H_2SO_4	-167	*Int. J. Energy Res.*, 2022, **46**, 17668-17681.
MoP/FeP/PCN	1 M KOH	-140	*Colloids Surf. A Physicochem. Eng. Asp.*, 2022, **636**, 128206.
	0.5 M H_2SO_4	-170	

References

1 X. Zhang, Z. Wu and D. Wang, *Electrochimica Acta*, 2018, **281**, 540-548. doi:10.1016/j.electacta.2018.05.176

2 C. Pi, C. Huang, Y. Yang, H. Song, X. Zhang, Y. Zheng, B. Gao, J. Fu, P. K. Chu and K. Huo, *Applied Catalysis B: Environmental*, 2020, **263**, 118358. doi:10.1016/j.apcatb.2019.118358

3 J. Kibsgaard and T. F. Jaramillo, *Angewandte Chemie International Edition*, 2014, **53**, 14433-14437. doi:10.1002/anie.201408222

4 Y. Ma, C.-X. Wu, X.-J. Feng, H.-Q. Tan, L.-K. Yan, Y. Liu, Z.-H. Kang, E.-B. Wang and Y.-G. Li, *Energy & Environmental Science*, 2017, **10**, 788-798. doi:10.1039/C6EE03768B

5 D. Zhao, K. Sun, W.-C. Cheong, L. Zheng, C. Zhang, S. Liu, X. Cao, K. Wu, Y. Pan, Z. Zhuang, B. Hu, D. Wang, Q. Peng, C. Chen and Y. Li, *Angewandte Chemie International Edition*, 2020, **59**, 8982-8990. doi:10.1002/ange.201908760